

Review

---

# Semileptonic and Missing Energy $B$ Decays at Belle II

---

Giovanni Gaudino

## Special Issue

Selected Papers from the 13th International Conference on New Frontiers in Physics (ICNFP 2024)

Edited by

Prof. Dr. Larissa Bravina, Prof. Dr. Sonia Kabana and Prof. Dr. Armen Sedrakian



*Review*

# Semileptonic and Missing Energy $B$ Decays at Belle II <sup>†</sup>

**Giovanni Gaudino**  on behalf of Belle II Collaboration

Scuola Superiore Meridionale, INFN Napoli, 80134 Naples, Italy; gaudino@na.infn.it

<sup>†</sup> This paper is based on the talk at the 13th International Conference on New Frontiers in Physics (ICNFP 2024), Crete, Greece, 26 August–4 September 2024.

**Abstract:** The Belle II experiment has collected a  $364 \text{ fb}^{-1}$  sample of collisions at the  $\Upsilon(4S)$  resonance. This dataset, with its low particle multiplicity and well-constrained initial state, provides an ideal environment for studying semileptonic and missing energy  $B$  decays. In this paper, I will present recent results on these decays, emphasizing their impact on the determination of CKM matrix elements and potential new physics. I will also discuss the techniques used for missing energy reconstruction and the challenges of signal-background discrimination. Future analysis prospects with larger datasets will also be highlighted.

**Keywords:** LFU; electroweak penguin; Belle II

## 1. Introduction

In the Standard Model (SM) of particle physics, the electroweak force carriers are expected to interact equally with all three charged leptons ( $e$ ,  $\mu$ , and  $\tau$ ), a principle referred to as lepton flavor universality (LFU) [1–4]. Semileptonic  $B$  decays provide rigorous tests of LFU, making them highly sensitive to potential deviations indicative of physics beyond the SM. A particularly important observable is the branching-fraction ratio:

$$R(H_{\tau/\ell}) = \frac{\mathcal{B}(B \rightarrow H\tau\nu_{\tau})}{\mathcal{B}(B \rightarrow H\ell\nu_{\ell})}, \quad (1)$$

where  $\ell$  represents an electron or muon, and  $H$  denotes a hadron. The hadron  $H$  can correspond to exclusive decay modes such as  $D^{(*)}$  or  $\pi$ , or represent an inclusive hadronic state  $X$ . This ratio is advantageous due to its partial cancellation of theoretical uncertainties (e.g., form factors) and experimental uncertainties (e.g., efficiencies), providing a robust test of LFU.

Semileptonic  $B$ -meson decays involving the  $b \rightarrow c\ell\nu_{\ell}$  transition are particularly sensitive to possible new interactions that violate LFU. Among these, the decay  $B \rightarrow D^*\ell\nu_{\ell}$  offers rich phenomenology through its angular distributions, enabling precise tests of LFU [5,6]. This decay is fully characterized by the recoil parameter  $w$  and three angular variables:  $\theta_{\ell}$ ,  $\theta_D$ , and  $\chi$ . The recoil parameter is defined as follows:

$$w = \frac{E_{D^*}}{m_{D^*}}, \quad (2)$$

where  $E_{D^*}$  is the energy of the  $D^*$  meson in the  $B$  rest frame, and  $m_{D^*}$  is the known mass of the  $D^*$  meson. The helicity angles are shown in Figure 1 and defined as follows:

- $\theta_{\ell}$ : the angle between the direction of the charged lepton in the virtual  $W$  boson frame and the  $W$  boson direction in the  $B$  rest frame;
- $\theta_D$ : the angle between the direction of the  $D$  meson in the  $D^*$  frame and the  $D^*$  meson direction in the  $B$  rest frame;



Academic Editors: Larissa Bravina, Sonia Kabana and Armen Sedrakian

Received: 10 March 2025

Revised: 13 April 2025

Accepted: 23 May 2025

Published: 4 June 2025

**Citation:** Gaudino, G., on behalf of Belle II Collaboration. Semileptonic and Missing Energy  $B$  Decays at Belle II. *Particles* **2025**, *8*, 60. <https://doi.org/10.3390/particles8020060>

**Copyright:** © 2025 by the author. Licensee MDPI, Basel, Switzerland. This article is an open access article distributed under the terms and conditions of the Creative Commons Attribution (CC BY) license (<https://creativecommons.org/licenses/by/4.0/>).

- $\chi$ : the angle between the decay planes of the virtual  $W$  boson and the  $D^*$  meson in the  $B$  rest frame.

This document presents the latest measurements of  $R(D^*)$  and  $|V_{ub}|$  performed by the Belle II experiment. Additionally, results on electroweak penguin  $B$  decays, such as  $B^+ \rightarrow K^+ \nu \bar{\nu}$ , are reported. The process  $B^+ \rightarrow K^+ \nu \bar{\nu}$  benefits from minimal hadronic uncertainties, providing a theoretically clean probe for new physics. The branching fraction of this decay can be significantly enhanced in models predicting high-mass non-SM particles, such as leptoquarks [7–9]. Furthermore, new low-mass undetectable exotic particles (e.g., dark matter candidates or mediators of a dark sector) may be produced alongside the kaon, leading to two-body or three-body decays with substantial missing energy.

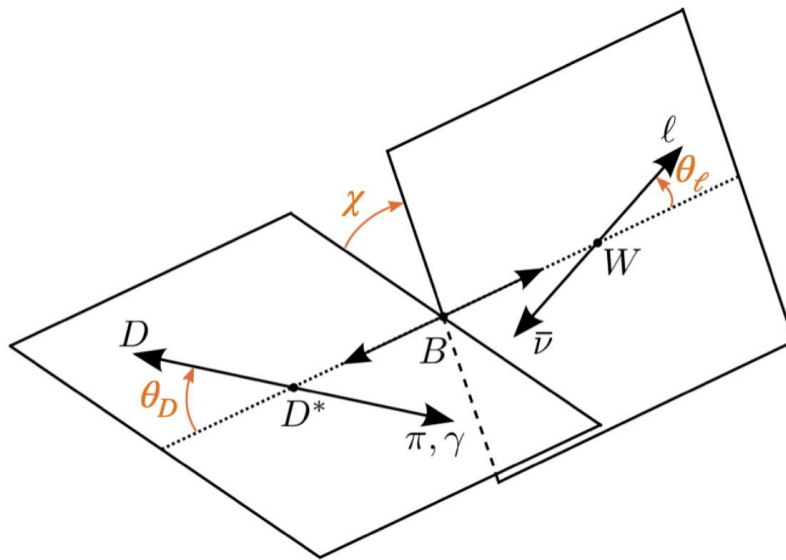


**Figure 1.** Kinematic configuration of the decay  $B \rightarrow D^{(*)} \ell \bar{\nu}_\ell$ , followed by  $D^* \rightarrow D \pi/\gamma$ . The angles  $\theta_\ell$ ,  $\theta_D$ , and  $\chi$  define the decay topology.

## 2. The Belle II Detector, Experimental Data, and MC Simulations

The Belle II experiment, situated at the SuperKEKB collider in Tsukuba, Japan, primarily collects data at the  $Y(4S)$  resonance to study  $B$  meson decays. The Belle II detector consists of several key components: the Vertex Detector (including a Pixel Detector (PXD) and a Silicon Vertex Detector (SVD)) for high-precision vertexing and tracking, the Central Drift Chamber (CDC) for momentum measurements, Time-Of-Propagation (TOP) counters and ring-imaging Cherenkov counters (ARICH) for particle identification, an Electromagnetic Calorimeter (ECL) for detecting electrons, photons, and neutral particles, and a Resistive Plate Chamber system (KLM) for muon and  $K_L$  detection.

The dataset used for these analyses comprises an integrated luminosity of  $364 \text{ fb}^{-1}$  collected from 2019 to 2022, except for the analysis explained in Section 3, where the luminosity is  $L = 189 \text{ fb}^{-1}$ . Experimental results are interpreted and compared with Standard Model predictions using Monte Carlo simulations, employing software packages such as EVTGEN [10], PYTHIA [11], and KKMC [12]. The full detector responses and simulations are executed with GEANT4, while data and Monte Carlo reconstructions are performed using the Belle II analysis software framework, basf2 [13].

### Full Event Interpretation: FEI

The Full Event Interpretation (FEI) [14] is an algorithm used in the Belle II experiment to classify events into signal-side (the  $B$  decay) and tag-side (the other  $B$  produced in the event). It provides crucial details about  $B$  decays, such as event type (e.g.,  $q\bar{q}$ ,  $\tau\tau$ , or  $B\bar{B}$ ),

decay vertex, and the reconstructed four-momentum of the tag and signal  $B$  mesons. FEI employs Multivariate Classifiers for each decay channel and is trained on Monte Carlo data within the `basf2` software package. The method, used with a hadronic tagging approach, offers high purity but limited tagging efficiency compared to semileptonic tagging. In all the analyses presented here, the hadronic tagging method is employed.

### 3. Measurement of $R(D_{\tau/\ell}^*)$ with Hadronic Tag

The first lepton flavor universality test presented here involves the measurement of the ratio  $R(D_{\tau/\ell}^*)$  [15], defined as  $\mathcal{B}(\bar{B} \rightarrow D^* \tau^- \bar{\nu}_\tau) / \mathcal{B}(\bar{B} \rightarrow D^* \ell^- \bar{\nu}_\ell)$ . For both the numerator and denominator, a single lepton is required in the final state to eliminate normalization effects via the ratio, causing the cancellation of numerous systematics; the  $\tau$  is only reconstructed in the fully leptonic decays ( $\tau \rightarrow \ell \nu \bar{\nu}$ ). Leptons are identified using likelihood ratios.

Charge conjugation is implied in all physical processes.

The hadronic component of the  $B$  decay is reconstructed through specific decay chains, suppressing the combinatorial background by imposing a requirement of no other charged particles in the event. The reconstruction uses  $D^* \rightarrow D^+ \pi^0$  and  $D^* \rightarrow D^0 \pi^0$  decay chains, each with 11 sub-decay modes.

Signal extraction is accomplished through a 2D maximum-likelihood fit in  $E_{\text{ECL}}$  and  $M_{\text{miss}}^2$ . The former represents the sum of the energy deposits in the calorimeter not associated with either  $B_{\text{tag}}$  or  $B_{\text{sig}}$ . The latter,  $M_{\text{miss}}^2$ , is the squared magnitude of the missing 4-momentum. Figure 2 illustrates the distributions of these variables for three different samples: the numerator of  $R(D_{\tau/\ell}^*)$ , the denominator, and the main background  $\bar{B} \rightarrow D^{**} \ell^- \bar{\nu}_\ell$ .

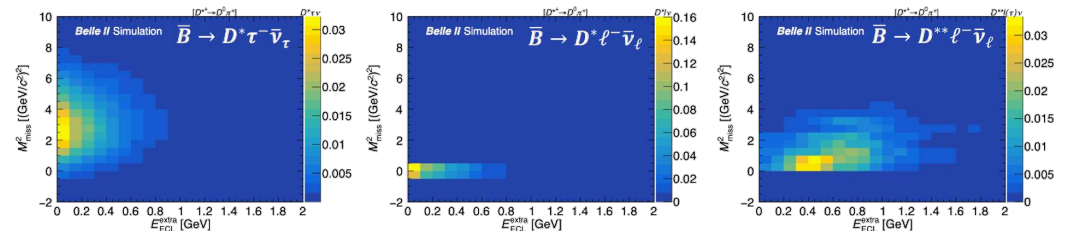


**Figure 2.**  $E_{\text{ECL}}$  vs.  $M_{\text{miss}}^2$  distribution of three different samples.  $\bar{B} \rightarrow D^* \tau^- \bar{\nu}_\tau$  is shown in the left plot,  $\bar{B} \rightarrow D^* \ell^- \bar{\nu}_\ell$  is in the center, and  $\bar{B} \rightarrow D^{**} \ell^- \bar{\nu}_\ell$  is in the right plot.

To validate and correct the shapes of the Probability Density Functions (PDFs) used in the fit and normalizations, three control samples are employed. Background contributions from misidentified  $D$  mesons are corrected in distinct  $M_{\text{miss}}^2$  regions using a sideband of the  $\Delta M = M_{D^*} - M_D$  variable. A correction of  $15 \pm 7$  MeV is applied to neutral cluster energies to address an observed excess at lower values in the control region with  $M_{\text{miss}}^2 < 1 \text{ GeV}^2$ . In the signal extraction fit, signal, normalization, and  $\bar{B} \rightarrow D^{**} \ell^- \bar{\nu}_\ell$  yields are left free, while background contributions from misidentified  $D$  mesons are constrained based on their calibration in the  $\Delta M$  control region. Other backgrounds are fixed according to their predicted branching fractions.

The result obtained is

$$R(D_{\tau/\ell}^*) = 0.267^{+0.041+0.028}_{-0.039-0.033} \quad (3)$$

The main sources of systematic uncertainty are MC statistics and the  $E_{\text{ECL}}$  shape. Our result is consistent with both the Standard Model prediction and the world average [16].

#### 4. Evidence of $B^+ \rightarrow K^+ \nu \bar{\nu}$ Decay

The Standard Model (SM) predicts the branching fraction of the  $B^+ \rightarrow K^+ \nu \bar{\nu}$  decay to be

$$\mathcal{B}(B^+ \rightarrow K^+ \nu \bar{\nu}) = (5.58 \pm 0.37) \times 10^{-6}, \quad (4)$$

as reported in [17]. However, models incorporating non-SM particles can significantly modify this prediction. Thus far, no experimental analyses have observed a signal, with the current upper limit on the branching fraction set at  $1.6 \times 10^{-5}$  at the 90% confidence level [18].

The Belle II experiment performed a measurement [19] using the full Run 1 dataset, employing two distinct methods: Inclusive Tagging Analysis (ITA) and Hadronic Tagging Analysis (HTA). The ITA method, known for its sensitivity, and the HTA method, a more conventional approach, were applied to nearly independent data samples.

The ITA method, designed for high precision, required the identification of the signal kaon candidate. Selection criteria included the smallest squared mass of the neutrino pair, defined as follows:

$$q_{\text{rec}}^2 = \frac{s}{4c^4} + M_K^2 - \sqrt{\frac{sE_K^*}{c^4}}, \quad (5)$$

assuming the signal  $B$  meson is at rest in the  $e^+e^-$  center-of-mass frame. Here,  $M_K$  denotes the mass of the  $K^+$  meson,  $E_K^*$  represents its reconstructed energy in the center-of-mass frame,  $\sqrt{s}$  is the center-of-mass energy, and  $c$  is the speed of light. Background suppression utilized event shape, kinematics, vertexing, and missing energy information through two Boosted Decision Trees (BDT1 and BDT2). A sample-composition fit in bins of the BDT2 output ( $\eta(\text{BDT2})$ ) and  $q_{\text{rec}}^2$  was employed to extract the signal branching fraction relative to the SM prediction (signal strength  $\mu$ ).

Various control samples validated the background modeling in simulated events, with systematic uncertainties and correction factors derived as needed. Key sources of systematic uncertainties included normalization of  $B\bar{B}$  backgrounds, limited simulated sample sizes, and modeling of specific decays such as  $B^+ \rightarrow K^+ K_L K_L$  and  $B \rightarrow D^{**} \ell \nu$ . Figure 3 shows the data in the signal regions for both ITA and HTA, overlaid with fit results.

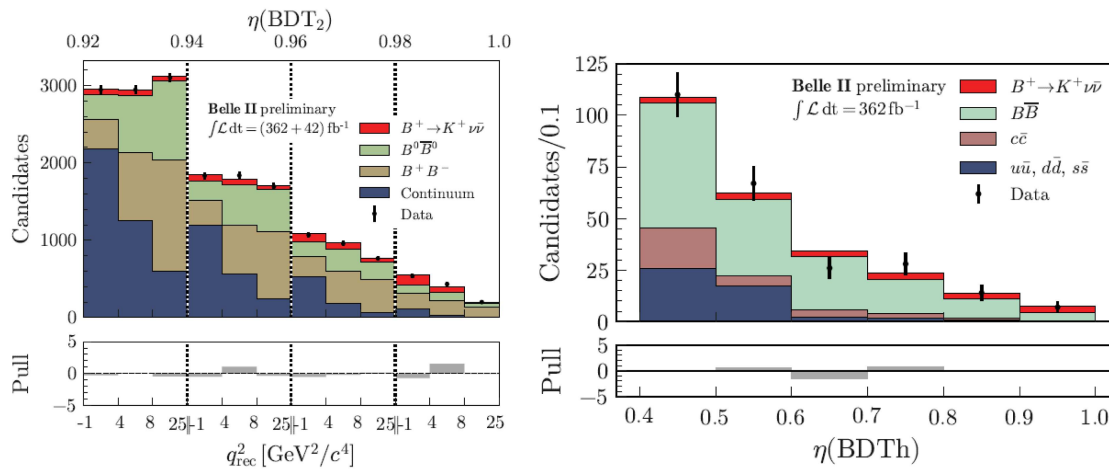


**Figure 3.** Observed yield and fit results in bins of  $\eta(\text{BDT2}) \times q_{\text{rec}}^2$  for ITA (left) and  $\eta(\text{BDTh})$  for HTA (right). The pull distributions are shown in the bottom panels.

The ITA approach was validated by measuring the branching fraction of  $B^+ \rightarrow \pi^+ K^0$  decay with minimal adaptation, yielding results consistent with the world average.

For HTA, signal extraction relied on the classifier output ( $\eta(\text{BDTh})$ ), achieving good agreement between data and fit. The ITA analysis yielded a signal strength of

$$\mu = 5.4 \pm 1.0 \text{ (stat)} \pm 1.1 \text{ (syst)}, \quad (6)$$

corresponding to a  $3.5\sigma$  excess over the background-only hypothesis and a  $2.9\sigma$  deviation from the SM expectation. The HTA results showed

$$\mu = 2.2^{+1.8}_{-1.7} \text{ (stat)}^{+1.6}_{-1.1} \text{ (syst)}, \quad (7)$$

indicating a  $1.1\sigma$  excess over the background-only hypothesis and a  $0.6\sigma$  deviation from the SM expectation. The ITA and HTA results were consistent within  $1.2\sigma$ . The combined signal strength was

$$\mu = 4.6 \pm 1.0 \text{ (stat)} \pm 0.9 \text{ (syst)}, \quad (8)$$

corresponding to a branching fraction:

$$\mathcal{B}(B^+ \rightarrow K^+ \nu \bar{\nu}) = [2.3 \pm 0.5 \text{ (stat)}^{+0.5}_{-0.4} \text{ (syst)}] \times 10^{-5}. \quad (9)$$

This represents the first evidence for  $B^+ \rightarrow K^+ \nu \bar{\nu}$  decay, with a significance of  $3.5\sigma$  above the background-only hypothesis and  $2.7\sigma$  above the SM expectation. Compared to previous results (see Figure 4), the ITA outcome agrees with prior hadronic-tag and inclusive measurements but shows a  $2\sigma$  tension with semileptonic  $B$ -tag results. HTA results are consistent with all previous measurements, representing the most precise determination using the hadronic tag method to date.

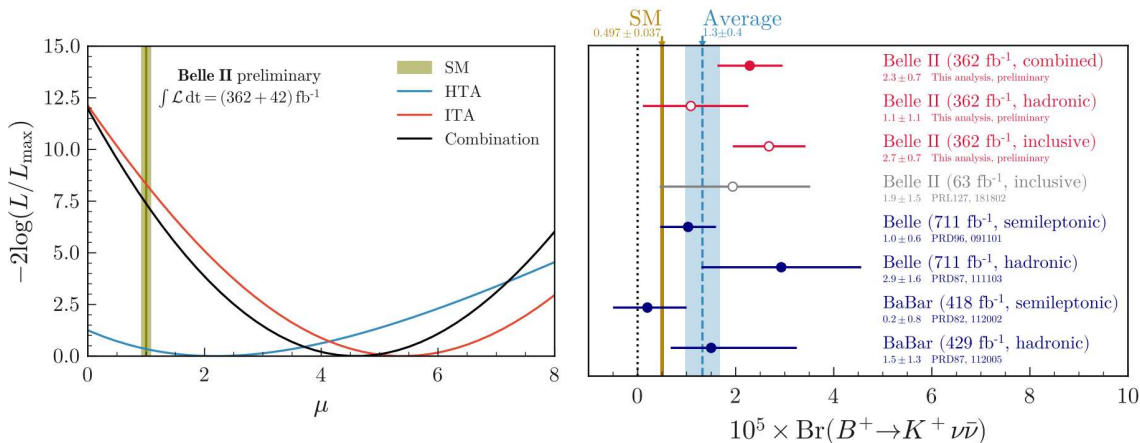


**Figure 4.** (Left):  $-2\log L$  for various  $\mu$  values from ITA, HTA, and combined analyses. (Right): Branching ratio measurements from this work compared with previous results and the SM prediction.

## 5. $|V_{ub}|$ Measurement from Simultaneous $B^0 \rightarrow \pi^- \ell^+ \nu_\ell$ and $B^+ \rightarrow \rho^0 \ell^+ \nu_\ell$ Analyses

Finally, we present our recent analysis aimed at determining the magnitude of the Cabibbo–Kobayashi–Maskawa (CKM) matrix element  $|V_{ub}|$ . Our study focuses on simultaneous measurements of the decay channels  $B^0 \rightarrow \pi^- \ell^+ \nu$  and  $B^+ \rightarrow \rho^0 \ell^+ \nu$ .

Our methodology involved the use of untagged measurements for both decay channels. By not employing flavor tagging, we simplify the experimental procedure and mitigate systematic uncertainties, thereby enhancing the precision of our measurements. In the untagged analysis, background suppression plays a critical role, as the number of events coming from the continuum  $e^+ e^- \rightarrow q\bar{q}$  is significantly higher than in hadronic

FEI analysis (as observed in previous sections). The other predominant background is the  $B \rightarrow X_c \ell \nu$  phenomenon.

The final fit to obtain the yields and the value of  $|V_{ub}|$  is performed using the variables  $M_{bc} = \sqrt{E_{beam}^{*2} - |\vec{p}_B^*|^2}$  and  $\Delta E = E_B^* - E_{beam}^*$  in  $q^2$  bins, where  $E_{beam}^*$ ,  $E_B^*$ , and  $\vec{p}_B^*$  represent the beam energy, reconstructed  $B$ -meson energy, and reconstructed  $B$ -meson momentum, all measured in the center-of-mass frame. We evaluated the systematic uncertainties, considering factors such as detector efficiency, signal and background modeling, and uncertainties in external parameters.

Our results yield a precise value for  $|V_{ub}|$ , which is consistent with current world averages and Standard Model predictions. The precise determination of  $|V_{ub}|$  contributes to a more comprehensive understanding of the CKM matrix and provides a stringent test of the Standard Model. Using this novel method, cross-feed signals between the two decay modes are properly accounted for. The partial branching fractions are determined from the fitted signal yields after efficiency corrections as a function of  $q^2$ . Furthermore, the total branching fraction is computed as the sum of these partial branching fractions, accounting for systematic correlations. As preliminary results, we obtain total branching fractions:

$$\mathcal{B}(B^0 \rightarrow \pi^- \ell^+ \nu_\ell) = (1.516 \pm 0.042 \text{ (stat)} \pm 0.059 \text{ (syst)}) \times 10^{-4} \quad (10)$$

and

$$\mathcal{B}(B^+ \rightarrow \rho^0 \ell^+ \nu_\ell) = (1.625 \pm 0.079 \text{ (stat)} \pm 0.180 \text{ (syst)}) \times 10^{-4} \quad (11)$$

These results are consistent with world averages, and the precision is comparable to previous measurements from Belle and *BABAR*.

To extract  $|V_{ub}|$ , the decay form factors for  $B^0 \rightarrow \pi^- \ell^+ \nu$  are parameterized using the Bourrely–Caprini–Lellouch (BCL) model [20], while the Bharucha–Straub–Zwicky (BSZ) parametrization [21] is used for  $B^+ \rightarrow \rho^0 \ell^+ \nu$ . Using  $\chi^2$  fits to the measured  $q^2$  spectra, we compute the following:

$$\chi^2 = \sum_{i,j=1}^N \frac{(\Delta B_i - \Delta \Gamma_i \tau)(\Delta B_j - \Delta \Gamma_j \tau)}{C_{ij}} + \sum_m \chi^2_{\text{Theory},m} \quad (12)$$

Incorporating constraints on non-perturbative hadronic contributions from lattice QCD calculations [22], we obtain the following preliminary result:

$$|V_{ub}| = (3.93 \pm 0.09 \pm 0.13 \pm 0.19) \times 10^{-3} \quad (13)$$

where the uncertainties are statistical, systematic, and theoretical, respectively.

The preliminary result from the  $B^+ \rightarrow \rho^0 \ell^+ \nu$  decay, including constraints from light-cone sum rule (LCSR) [23], is

$$|V_{ub}| = (3.19 \pm 0.12 \pm 0.17 \pm 0.26) \times 10^{-3} \quad (14)$$

The  $|V_{ub}|$  values obtained from the  $B^0 \rightarrow \pi^- \ell^+ \nu$  mode are consistent with previous exclusive measurements. Figure 5 shows the measured and fitted differential rates for  $B^0 \rightarrow \pi^- \ell^+ \nu$  and  $B^+ \rightarrow \rho^0 \ell^+ \nu$ , as well as the one-, two-, and three-standard-deviation uncertainty bands from the fits.

The result from the  $B^+ \rightarrow \rho^0 \ell^+ \nu$  mode is lower but remains consistent with previous experimental determinations from  $B \rightarrow \rho \ell \nu$  decays. In both cases, the precision is limited by theoretical uncertainties.

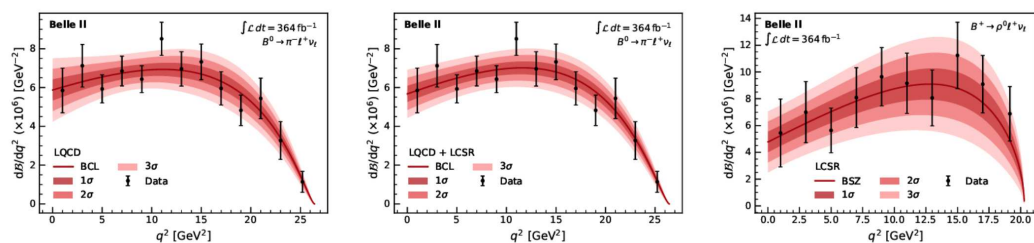


**Figure 5.** Ref. [24] Measured partial branching fractions as a function of  $q^2$  for  $B^0 \rightarrow \pi^- \ell^+ \nu_\ell$  (left, center) and  $B^+ \rightarrow \rho^0 \ell^+ \nu_\ell$  (right). The fitted differential rates are shown together with the one-, two-, and three-standard-deviation uncertainty bands for fits using constraints on the form factors from (left) LQCD, (center) LQCD and LCSR, and (right) LCSR predictions.

## 6. Summary and Future Prospects

These measurements represent significant steps towards precise testing of the Standard Model’s lepton universality hypothesis. The results are currently in line with both the Standard Model and world averages. The Belle II experiment, leveraging the capabilities of the SuperKEKB collider, is expected to reduce systematic uncertainties in future measurements. This will be achieved through increased data volumes and improved theoretical models, including better understanding and incorporation of effects like  $D \rightarrow K_L X$  decays. Future work includes extending these analyses to different decay channels, higher precision in lepton identification, and exploring other potential signs of new physics beyond the Standard Model.

**Funding:** This research received no external funding.

**Conflicts of Interest:** The authors declare no conflict of interest.

## References

1. Banerjee, S.; Ben-Haim, E.; Bernlochner, F.; Bertholet, E.; Bona, M.; Bozek, A.; Bozzi, C.; Brodzicka, J.; Chobanova, V.; Chrzaszcz, M.; et al. Averages of  $b$ -hadron,  $c$ -hadron, and  $\tau$ -lepton properties as of 2023. *arXiv* **2024**, arXiv:2411.18639.
2. de Barbaro, P.; Barnett, B.A.; Barbaro-Galtieri, A.; Barnes, V.E.; Baumann, T.; Bedeschi, F.; Behrends, S.; Belforte, S.; Bellettini, G.; Bellinger, J.; et al. Measurement of the ratio  $B(W \rightarrow \tau\nu)/B(W \rightarrow e\nu)$  in  $p\bar{p}$  collisions at  $\sqrt{s} = 1.8$  TeV. *Phys. Rev. Lett.* **1992**, *68*, 3398–3402. [[CrossRef](#)]
3. ATLAS Collaboration. Test of the universality of  $\tau$  and  $\mu$  lepton couplings in  $W$ -boson decays with the ATLAS detector. *Nat. Phys.* **2021**, *17*, 813–818. [[CrossRef](#)]
4. CMS Collaboration. Precision measurement of the  $W$  boson decay branching fractions in proton-proton collisions at  $\sqrt{s} = 13$  TeV. *Phys. Rev. D* **2022**, *105*, 072008. [[CrossRef](#)]
5. Adachi, I.; Adamczyk, K.; Aggarwal, L.; Aihara, H.; Akopov, N.; Aloisio, A.; Ky, N.A.; Asner, D.; Atmacan, H. Tests of Light-Lepton Universality in Angular Asymmetries of  $B^0 \rightarrow D^{*-} \ell \nu$  Decays. *Phys. Rev. Lett.* **2023**, *131*, 181801. [[CrossRef](#)]
6. Bobeth, C.; Bordone, M.; Gubernari, N.; Jung, M.; van Dyk, D. Lepton-flavour non-universality of  $\bar{B} \rightarrow D^* \ell \bar{\nu}$  angular distributions in and beyond the Standard Model. *Eur. Phys. J. C* **2021**, *81*, 984. [[CrossRef](#)]
7. Bernlochner, F.U.; Sevilla, M.F.; Robinson, D.J.; Wormser, G. Semitauonic  $b$ -hadron decays: A lepton flavor universality laboratory. *Rev. Mod. Phys.* **2022**, *94*, 015003. [[CrossRef](#)]
8. Bigi, D.; Gambino, P. Revisiting  $B \rightarrow D \ell \nu$ . *Phys. Rev. D* **2016**, *94*, 094008. [[CrossRef](#)]
9. Gambino, P.; Jung, M.; Schacht, S. The  $V_{cb}$  puzzle: An update. *Phys. Lett. B* **2019**, *795*, 386–390. [[CrossRef](#)]
10. Lange, D.J. The EvtGen particle decay simulation package. *Nucl. Instrum. Meth. A* **2001**, *462*, 152–155. [[CrossRef](#)]
11. Sjöstrand, T.; Ask, S.; Christiansen, J.R.; Corke, R.; Desai, N.; Ilten, P.; Mrenna, S.; Prestel, S.; Rasmussen, C.O.; Skands, P.Z. An introduction to PYTHIA 8.2. *Comput. Phys. Commun.* **2015**, *191*, 159–177. [[CrossRef](#)]
12. Jadach, S.; Ward, B.F.L.; Was, Z. The Precision Monte Carlo event generator K K for two fermion final states in  $e^+e^-$  collisions. *Comput. Phys. Commun.* **2000**, *130*, 260–325. [[CrossRef](#)]
13. Kuhr, T.; Pulvermacher, C.; Ritter, M.; Hauth, T.; Braun, N. The Belle II Core Software. *Comput. Softw. Big Sci.* **2019**, *3*, 1. [[CrossRef](#)]

14. Keck, T.; Abudinén, F.; Bernlochner, F.U.; Cheaib, R.; Cunliffe, S.; Feindt, M.; Ferber, T.; Gelb, M.; Gemmler, J.; Goldenzweig, P.; et al. The Full Event Interpretation: An Exclusive Tagging Algorithm for the Belle II Experiment. *Comput. Softw. Big Sci.* **2019**, *3*, 6. [[CrossRef](#)]
15. Adachi, I.; Adamczyk, K.; Aggarwal, L.; Ahmed, H.; Aihara, H.; Akopov, N.; Aloisio, A.; Ky, N.A.; Asner, D.M.; Atmacan, H.; et al. A test of lepton flavor universality with a measurement of  $R(D^*)$  using hadronic  $B$  tagging at the Belle II experiment. *arXiv* **2024**, arXiv:2401.02840. [[CrossRef](#)]
16. Amhis, Y.; Banerjee, S.; Ben-Haim, E.; Bertholet, E.; Bernlochner, F.U.; Bona, M.; Bozek, A.; Bozzi, C.; Brodzicka, J.; Chobanova, V.; et al. Averages of b-hadron, c-hadron, and  $\tau$ -lepton properties as of 2021. *Phys. Rev. D* **2023**, *107*, 052008. [[CrossRef](#)]
17. Parrott, W.G.; Bouchard, C.; Davies, C.T.H. Standard Model predictions for  $B \rightarrow K\ell^+\ell^-$ ,  $B \rightarrow K\ell_1^-\ell_2^+$ , and  $B \rightarrow K\nu\bar{\nu}$  using form factors from  $N_f = 2 + 1 + 1$  lattice QCD. *Phys. Rev. D* **2023**, *107*, 119903. [[CrossRef](#)]
18. Particle Data Group; Workman, R.L.; Burkert, V.D.; Crede, V.; Klempert, E.; Thoma, U.; Tiator, L.; Agashe, K.; Aielli, G.; Allanach, B.C. Review of Particle Physics. *Prog. Theor. Exp. Phys.* **2022**, *2022*, 083C01. [[CrossRef](#)]
19. Adachi, I.; Adamczyk, K.; Aggarwal, L.; Ahmed, H.; Aihara, H.; Akopov, N.; Aloisio, A.; Ky, N.A.; Asner, D. Evidence for  $B^+ \rightarrow K^+\nu\bar{\nu}$  decays. *Phys. Rev. D* **2024**, *109*, 112006. [[CrossRef](#)]
20. Bourrely, C.; Caprini, I.; Lellouch, L. Model-independent description of  $B \rightarrow \pi\ell\nu$  decays and a determination of  $|V_{ub}|$ . *Phys. Rev. D* **2009**, *79*, 013008. [[CrossRef](#)]
21. Bharucha, D.; Rey, S.J.; Straub, L. Precision predictions in exclusive semileptonic  $B$  decays using light-cone sum rules. *J. High Energy Phys.* **2016**, *08*, 098. [[CrossRef](#)]
22. Aoki, Y.; Blum, T.; Collins, S.; Debbio, L.D.; Morte, M.D.; Dimopoulos, P.; Feng, X.; Golterman, M.; Gottlieb, S.; Gupta, R.; et al. [Flavour Lattice Averaging Group (FLAG)]. *arXiv* **2024**, arXiv:2411.04268.
23. Hammad, A.; Ko, P.; Lu, C.T.; Park, M. Exploring exotic decays of the Higgs boson to multi-photons at the LHC via multimodal learning approaches. *JHEP* **2024**, *09*, 166. [[CrossRef](#)]
24. Adachi, I.; Aggarwal, L.; Aihara, H.; Akopov, N.; Aloisio, A.; Althubiti, N.; Ky, N.A.; Asner, D.M.; Atmacan, H.; Aushev, T.; et al. Determination of  $|V_{ub}|$  from simultaneous measurements of untagged  $B^0 \rightarrow \pi^-\ell^+\nu_\ell$  and  $B^+ \rightarrow \rho^0\ell^+\nu_\ell$  decays. *arXiv* **2024**, arXiv:2407.17403.

**Disclaimer/Publisher’s Note:** The statements, opinions and data contained in all publications are solely those of the individual author(s) and contributor(s) and not of MDPI and/or the editor(s). MDPI and/or the editor(s) disclaim responsibility for any injury to people or property resulting from any ideas, methods, instructions or products referred to in the content.